JOURNAL OF MATERIALS SCIENCE **38** (2003) 1925–1930

Recrystallized grain size prediction in a particulate reinforced metal matrix composite

M. FERRY*, P. R. MUNROE
School of Materials Science and Engineering, University of New South Wales, Sydney NSW 2052, Australia
E-mail: m.ferry@unsw.edu.au

The recrystallized grain size following cold rolling and annealing of an Al alloy (AA2014) and a particulate reinforced AA2014 composite was investigated. The composite contained 20 vol% alumina particulates of average diameter 15 μm. The recrystallized grain size in the composite was finer than in the alloy, for a given set of conditions; this was most notable for material strained less than 50% cold-work. This behaviour was attributable to a higher nucleation efficiency in the matrix adjacent to coarse alumina particles in the composite. A model was presented for the composite to predict the recrystallized grain size as a function of strain, with respect to the size distribution and number density of alumina particles. This model predicted the strain dependence of the recrystallized grain size and, in particular, the grain size insensitivity to strain at moderate-to-high levels of cold-work. © *2003 Kluwer Academic Publishers*

1. Introduction

Since the 1980's, considerable effort has been directed towards understanding the mechanical and physical behaviour of discontinuously reinforced metal matrix composites (MMCs) containing either whiskers, platelets or particulates, since these materials often have mechanical properties superior to their unreinforced alloy counterparts and approaching that of continuous-fibre reinforced MMCs [1–6]. One of the prime advantages of discontinuously reinforced MMCs is that billets of the composite can be mechanically processed using technologies developed for monolithic alloys; for example, extrusion, forging or hot and cold rolling [1–15].

The basic structural difference between discontinuously reinforced composites and their alloys is that the volume fraction of the reinforcement phase is usually considerably higher (up to 30 vol%) than the particle content of the unreinforced alloys ($\sim$<5 vol%). It is accepted that the presence of the reinforcing phase affects both the deformation and annealing behaviour of the metal matrix by enhancing nucleation of recrystallized grains in zones of high plastic strain generated by deformation (see e.g. [1, 10, 16]). Hence, the reinforcing phase will also affect the rate of recrystallization, recrystallized grain size and recrystallization texture [16], and may also limit grain growth. The aim of the present work is to examine the effect of the reinforcement phase on the recrystallized grain size of a cold rolled alumina particulate reinforced metal matrix composite (PMMC).

2. Experimental

An aluminium alloy (AA 2014) PMMC containing 20 vol% alumina particles of average diameter 15 μm, together with an unreinforced AA 2014 alloy, was used. The composite was produced by Alcan International Limited, Kingston, Canada via a molten metal mixing route and then cast and processed to produce 15 mm thick plate. The alloy and composite were solution treated at 505°C and cold rolled to 20% reduction and annealed for 20 h at 350°C to produce a low solute aluminium matrix with a dispersion of coarse (>1 μm), equiaxed $CuAl_2$ (θ) precipitates. The materials also contain a small volume fraction of coarse (>1 μm) $(Fe,Mn)_3SiAl_{12}$ constituent particles [10]. Fig. 1 shows optical micrographs of both the alloy and composite showing the dispersion of both constituent and alumina particles.

Following the initial heat treatment, cold rolling of both the alloy and composite was carried out using a two-high laboratory mill by successive reductions of 5–10% per pass to strains up to 95% reduction. Following cold rolling, samples were annealed at times from 10^1–10^4 s at temperatures to 500°C until fully recrystallized.

Specimens for optical metallography were mounted in cold-setting resin, mechanically ground and polished to produce clean metallographic surfaces with minimal surface relief. To observe the distribution of constituent particles, specimens were etched for 10–20 s in Keller's reagent. To observe the recrystallized microstructure, specimens were anodised using Barker's reagent and

* Author to whom all correspondence should be addressed.

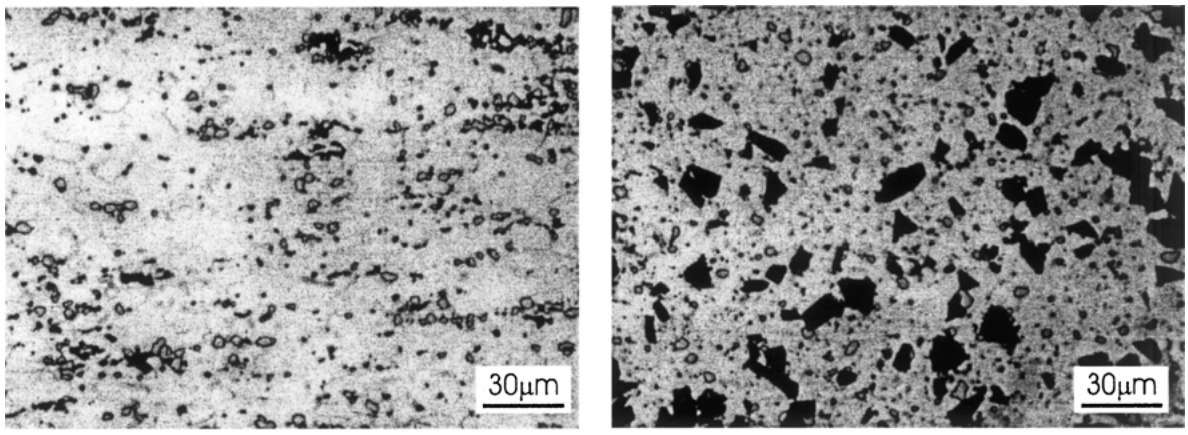

Figure 1 Optical micrographs of the (a) alloy and (b) composite showing the size, shape and distribution both of the constituent particles and alumina particulates.

the average grain size, for a given processing condition, was determined by the linear intercept method. Specimens for transmission electron microscopy (TEM) were sliced from both the alloy and composite parallel to the ND-TD plane. Thin foils were jet polished to perforation with a Struers Tenupol polishing system using 20% nitric acid in methanol at a temperature of −30°C. The foils were examined in a JEOL 2000FX TEM, operating at 200 kV.

3. Results and discussion

3.1. Variables affecting recrystallized grain size

The recrystallized grain size as a function of the degree of cold-work and annealing temperature is given in Fig. 2 for both the alloy and composite. Several points are worth noting. First, there exists a critical strain below which complete recrystallization did not occur in both materials. This strain was slightly lower in the composite (∼<3%) compared with the alloy (∼5%). Second, following deformation to strains slightly greater than the critical level of cold-work, both materials recrystallized to a large grain size ($d > 100$ μm). For the alloy, the grain boundaries of these coarse recrystallized grains were regular (Fig. 3a), whereas the grain boundaries of the composite were slightly irregular (Fig. 3b). Third, with increasing strain, the recrystallized grain size decreased in both materials, but the rate of decrease in grain size with increasing strain was greater for the composite than for the alloy. Therefore, for a given level of strain, the grain size in the composite was finer than in the alloy, but as the level of cold-work increased, the difference in the recrystallized grain size between the two materials became negligible. Fourth, the recrystallized grain size in the composite was largely independent of temperature. Consistent with this work, Vyletel *et al.* [17] observed similar behaviour in a 2219–15 vol%-1.7 μm-TiC particulate composite, although they did not compare the behaviour of this composite with the unreinforced alloy.

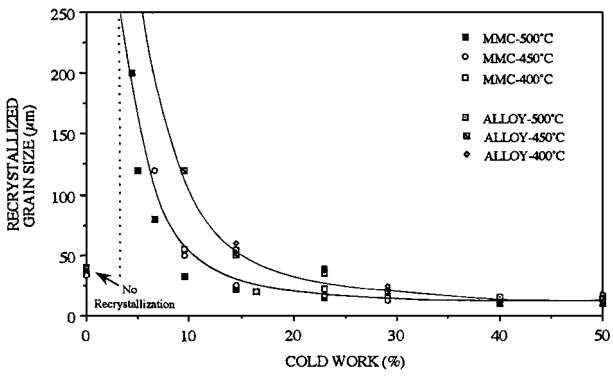

Figure 2 Recrystallized grain size of the alloy and composite as a function of strain.

For the alloy, nucleation of recrystallized grains was associated with either constituent particles or grain boundaries, whereas the alumina particles in the composite provide additional sites for nucleation (Fig. 4). These additional sites will tend to increase the nucleation efficiency for a given level of strain, and a finer grain size will be produced The enhanced nucleation in the composite may be explained by the model of Humphreys [18] whereby the critical particle size, d_c, for particle stimulated nucleation (PSN) decreases with increasing strain. Thus, for a given strain, the large alumina particles in the composite are more likely to nucleate new grains than the smaller constituent particles in the alloy. For the alumina particles, d_c remains well below the average diameter of these particles ($d = 15$ μm), even at low strains ($\varepsilon < 20\%$), and extensive PSN is likely to occur. In contrast, constituent particles in the alloy are less than d_c, even at moderate strains ($\varepsilon = 50\%$), and hence nucleation at individual particles would not be extensive. The inability of these constituent particles to nucleate grains at low strains may explain the gradual decrease in grain size with increasing strain for the alloy. Conversely, the greater number of viable nucleation sites in the composite resulted in a sharp decrease in grain size at low strain ($\varepsilon < 20\%$), and the relative insensitivity to strain thereafter.

Following higher strains ($\varepsilon > 50\%$), many of the particles in the alloy are likely to be large enough for extensive PSN to occur. Subsequently, the nucleation rate in the alloy was comparable to that of the

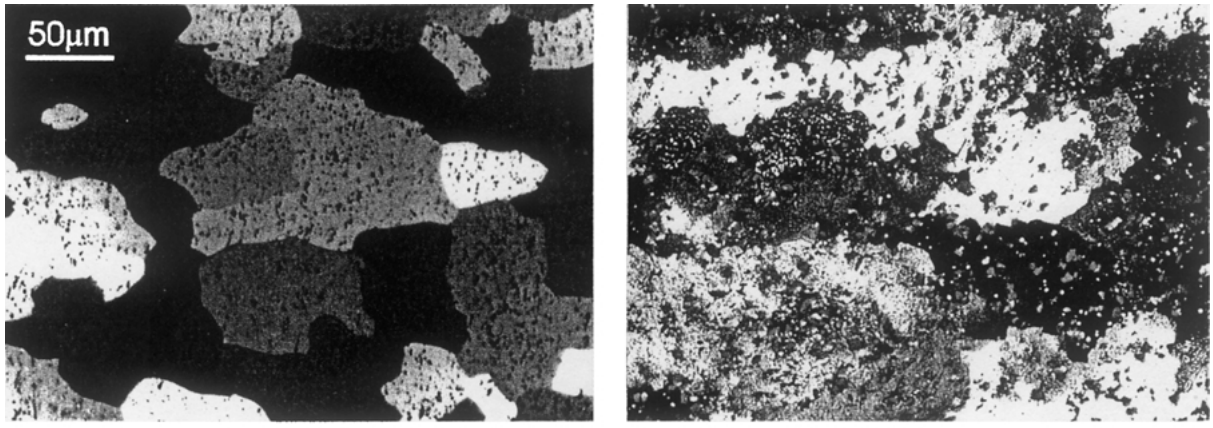

Figure 3 Optical micrographs of the (a) alloy and (b) composite following 9% strain and annealing at 500°C.

Figure 4 Nucleation of recrystallized grains at a cluster of alumina particles following annealing for 100 s at 260°C ($\varepsilon = 50\%$).

composite at high strains, and the recrystallized grain size approached similar values in both materials.

3.2. Recrystallized grain size prediction

The alumina particles in the composite refined the recrystallized grain size by enhancing nucleation of recrystallization of the matrix in their vicinity [16]. Since nucleation occurred predominantly near alumina particles, it may be possible to calculate the recrystallized grain size if the number and size distribution of these particles is known. A model is presented for the composite to predict the recrystallized grain size as a function of strain. The model rests on the assumption that nucleation is restricted to the deformation zones surrounding large particles (see e.g. [19, 20]).

3.2.1. Description of the model

To calculate the recrystallized grain size from the number of potential nucleation sites in the matrix, the recrystallization kinetics first need to be established. In materials where recrystallized grains originate at well-defined sites, the KJMA theory should apply [16, 21]. There are two extreme cases for predicting the recrystallized grain size on the basis of this theory, that is, steady state nucleation or site saturated nucleation [20]. For the case where nucleation is site-saturated, the recrystallized grain size D_r may be determined directly from the total number of potential nucleation sites using:

$$D_r = [N_V(d_c)]^{1/3} \quad (1)$$

Thus, the density of nucleation sites and, hence, the recrystallized grain size, simply depends on the number of particles in the total population with diameters greater than d_c, that is $N_V(d_c)$. This parameter is a function of the degree of cold-work since d_c is related to the level of strain, so it should be possible to calculate the recrystallized grain size as a function of strain. In the model, several assumptions are made:

- Site-saturated transformation kinetics applies [21], whereby all nuclei form at the same time and grow at the same rate. This assumption is valid for aluminium alloys containing a high volume fraction of coarse particles [16].
- Nucleation occurs at each of the alumina particles in the total size distribution that have sizes greater than d_c. Alternative nucleation sites are assumed to be negligibly small compared with the number of alumina particles greater than d_c. This is the case for the composite.

- Neither the constituent particles nor alumina particles impede the growth of those nuclei that form. This assumption is reasonable since the driving force for recrystallization is considerably greater than the pinning force exerted by very large particles [16]. Nevertheless, Fig. 3b shows that grain boundaries in the composite are more irregular than that observed in the alloy which indicates that some grain boundary/particle interaction does occur.

3.2.2. Application of the model

To model the recrystallized grain size as a function of the degree of cold-work, it was necessary to first determine both the size distribution of the alumina particles and the number of particles per unit volume of microstructure. To evaluate D_r the following calculations were carried out:

(i) The number of alumina particles per unit area (N_A) and their size distribution were determined using image analysis in conjunction with a JEOL 6400 SEM. Ten randomly-selected fields were analysed at 500× magnification and the results combined to determine both N_A and size distribution, the latter computed on the assumption that the particles are spherical. Fig. 5 shows the cumulative frequency distribution of particle size which indicates that the size distribution is close to log-normal with a mean particle diameter of ~15 μm.

(ii) Based on the model by Sandström [22], d_c was determined as a function of degree of cold work. Sandström proposed that $\lambda + d_c/2 > r_c = 2\gamma/\tau\rho$ where λ is the width of the deformation zone, r_c is the critical nucleus radius, γ is grain boundary energy, τ the dislocation line tension and ρ is the matrix dislocation density. The critical particle diameter may also be expressed in terms of matrix subgrain diameter, D_{sg}, as $d_c = 4\gamma_b D_{sg}/3\gamma_s$ [16] where γ_b is the boundary energy of the nucleus and γ_s is the matrix subgrain boundary energy. These equations are essentially equivalent and since both ρ and D_{sg} are strain dependent, so is the critical diameter, d_c (Table I) The present model utilises the relationship between d_c and strain given by Sandström for aluminium [22] which showed a good correlation with the results of PSN in a cold deformed Al-Si alloy [18].

(iii) To calculate $N_V(d_c)$, the spatial size distribution of the total population of alumina particles must first be determined. This 3-D distribution was readily determined from the 2-D distribution using the Schwartz-Saltykov procedure [23]. The transformation from N_A to N_V for a given particle size class d_j is given in Table I.

(iv) Using the values of d_c, determined for a given level of strain (Table I), the total number of particles per unit volume greater than the critical particle diameter ($N_V(d_c)$ was calculated for each particle size class d_j.

(v) Finally, D_r, for a given value of d_c, was calculated using Equation 1. Since D_r is uniquely related to d_c, this allows D_r to be related to the degree of cold-work. The calculation to generate D_r as a function of degree of cold-work is given in Table I.

3.2.3. Comparison with experiment

The predicted grain size (D_r) as a function of strain is given by the curve in Fig. 6. It may be seen that D_r increases only slightly with decreasing strain, and more sharply for strains below ~25% cold-work. Also given in Fig. 6 are measured recrystallized grain sizes for a wide range of processing conditions (strain, heating rate, annealing temperature [24]). The actual grain diameter was determined from the linear intercept grain size ($\bar{l}$) using $D_r = 1.5\,\bar{l}$ which is often used to convert $\bar{l}$ to the actual grain diameter [25]. It is clear from Fig. 6 that a good correlation exists between the measured and

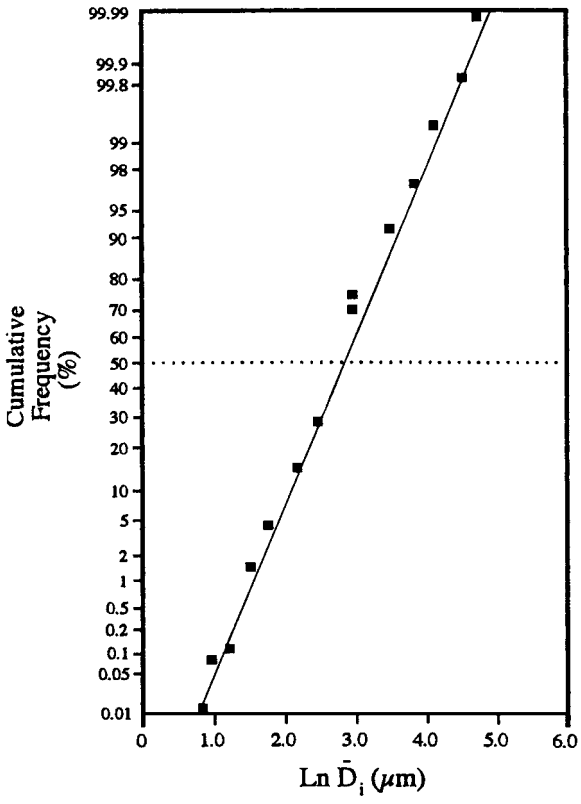

Figure 5 Log-probability frequency size distribution of alumina particles in the composite.

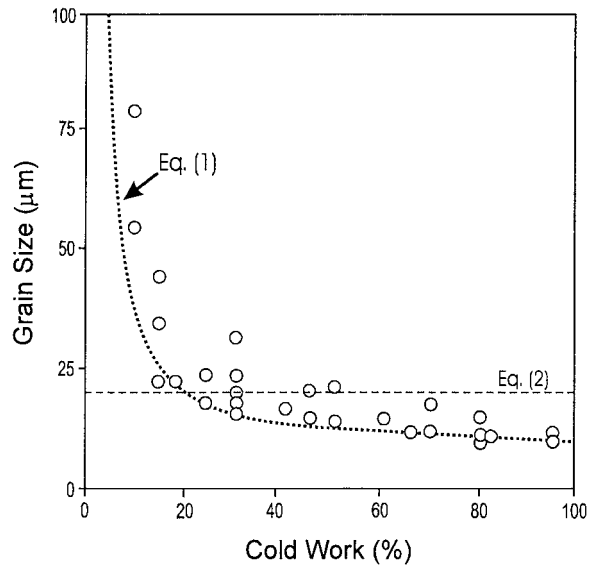

Figure 6 Predicted recrystallized grain size as a function of cold work in the composite. Data correspond to the measured grain size for a wide range of processing conditions.

TABLE I Calculations to predict the recrystallized grain size, D_r, as a function of degree of cold work

Planar size distribution $d_i(\mu m)$	Size groups	Number of particles/ mm^2 N_A	$d_i(\mu m)$ (From Ref. [23])	Number of particles/ mm^3 N_V	Critical particle diameter d_c (μm)	Strain corresponding to d_c [22] (%)	Predicted grain diameter D_r (μm)
0–2	<2	3428	2	634647	2	70	9.7
2–4	2–6	1420	6	295282	4	50	13.0
4–6							
6–8	6–10	900	10	106434	8	26	18.7
8–10							
10–12	10–14	392	14	38417	12	16	27.9
12–14							
14–16	14–18	62	18	4060	16	14	51.0
16–18							
18–20	18–22	51	22	1815	20	10	67.0
20–22							
22–24	22–26	31	26	414	24	7	87.1
24–26							
26–28	26–30	17	30	1100	28	4	96.9
28–30							
>30	>30	17	–	1082169	–	–	

predicted grain size using Equation 1. Despite the simplicity of the model, it is able to predict the observed strain insensitivity of the recrystallized grain size for the composite in the same regime of strain where the grain size in the alloy was decreasing significantly.

The prediction of recrystallized grain size in PMMCs has also been made using a relation of the form [4]:

$$D_r = \bar{d}_p(1 - f)^{1/3}/f^{1/3} \quad (2)$$

where $\bar{d}_p$ is the average particulate diameter and f the particulate volume fraction of particulate. Given that $\bar{d}_p = 15\ \mu$m and $f = 0.2$ for the composite, the recrystallized grain size predicted from Equation 2 is given in Fig. 6. Equation 2 corresponds reasonably well with the observed grain size for strains greater than ~20% cold work, that is, where nucleation at each particle is expected to occur.

Despite the close correlation between the current model and experiment, the model is dependent on the accuracy to which some of the measurements are made. Furthermore, several of the assumptions cannot be satisfied fully for PMMCs. For example, the Schwartz-Saltykov transformation is based on the assumption that the particles are spherical and dispersed randomly [23]. This is not satisfied entirely for the composite as the optical micrograph in Fig. 1b shows both particle clustering and angular-shaped particles. The inherent clustering of alumina particles will change the *effective* critical particle size and alter $N_V(d_c)$, as nucleation may occur preferentially at these clusters (Fig. 3). Furthermore, multiple nucleation can occur at large (>10 μm) particles [27] and, for the case of more angular particles, nucleation often occurs preferentially at sharp edges [27]. These associated effects will alter the values of N_V essential for calculating the recrystallized grain size. Additionally, constituent particles were not taken into account, and these particles will also act as nucleation sites at higher strains.

Fig. 7 shows the distribution of nearest-neighbour-distance between alumina particles (interparticulate spacing distribution [26]). This distribution is close to that expected for a random distribution of particles of varying sizes, that is, a Poisson distribution. However, a salient feature of the experimentally-determined distribution is the spike in the frequency histogram at small particle separations (<5 μm) which is an indication of particle clustering. Fig. 7 includes the linear intercept grain size distribution [26] of a fully recrystallized composite following 50% cold work and annealing for 30 s at 500°C. It can be seen that both distributions are comparable and indicates that the particulate dispersion is an important variable governing the recrystallized grain size distribution after moderate-to-high levels of cold work.

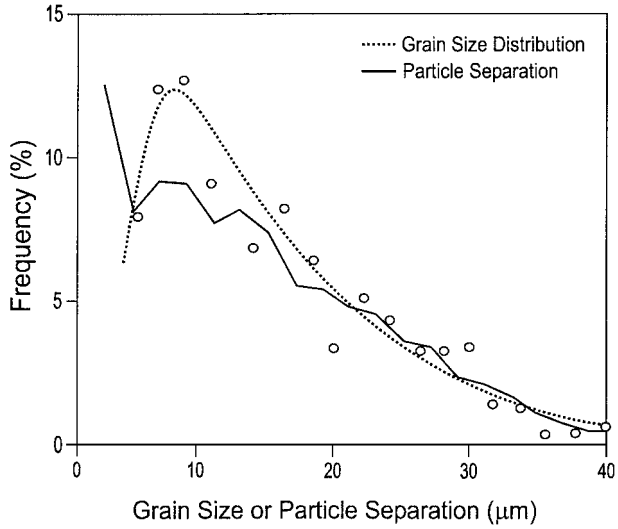

Figure 7 Frequency distribution of interparticulate spacing in the composite (unbroken curve), together with linear intercept grain size distribution (dashed curve) following annealing for 30 s at 500°C ($\varepsilon = 50\%$) (open symbols denote the percentage of grains below a given size for 2 μm intervals).

4. Conclusions

The addition of a high volume fraction of coarse alumina particles to an aluminium alloy altered the matrix

deformation behaviour during cold rolling and, for a given strain, refined the recrystallized grain size by enhanced nucleation at these particles. A model was presented for the composite to predict the recrystallized grain size as a function of strain, with respect to the size distribution and number density of alumina particles. This model successfully predicted the strain dependence of the recrystallized grain size and, in particular, the relative grain size insensitivity to strain at moderate-to-high levels of cold work. Despite this good correlation, the model is limited by the heterogeneity of the particulate distribution.

Acknowledgements

The authors express their gratitude to Dr David Lloyd of Alcan International Limited, Canada for supplying the composite.

References

1. T. W. CLYNE and P. J. WITHERS, "Introduction to Metal Matrix Composites" (Cambridge University Press, 1995).
2. D. J. LLOYD, *Int. Mater. Rev.* **39** (1994) 1.
3. J. W. MILLER and F. J. HUMPHREYS, *Scripta Metall.* **25** (1991) 33.
4. F. J. HUMPHREYS, in Proc. 9th Int. Risø Symp., Risø National Laboratories, Roskilde (1988) p. 51.
5. F. J. HUMPHREYS, W. S. MILLER and M. R. DJAZEB, *Mater. Sci. Tech.* **6** (1990) 1139.
6. B.-C. KO, G. S. PARK and Y.-C. YOO, *J. Mater. Proc. Tech.* **95** (1999) 210.
7. Y. L. LIU, N. HANSEN and D. JUUL JENSEN, *Metall. Trans* A **20** (1989) 1743.
8. Y. L. LIU, D. JUUL JENSEN and N. HANSEN, *ibid.* **23** (1992) 807.
9. B. V. RADHAKRISHNA Y. R. MAHAJAN and Y. V. R. K. PRASAD, *Metall. Mater. Trans* A **31** (2000) 629.
10. M. FERRY, P. R. MUNROE, A. CROSKY and T. CHANDRA, *Mater. Sci. Tech.* **8** (1992) 43.
11. M. FERRY and P. R. MUNROE, *ibid.* **11** (1995) 663.
12. *Idem.*, *ibid.* **11** (1995) 734.
13. B.-C. KO and Y.-C. YOO, *Comp. Sci. Tech.* **58** (1998) 479.
14. R. A. SHAHANI and T. W. CLYNE, *Mater. Sci. Eng.* A **135** (1991) 281.
15. C. A. STANFORD-BEALE and T. W. CLYNE, *Comp. Sci. Tech.* **35** (1989) 121.
16. F. J. HUMPHREYS and M. HATHERLY, "Recrystallization and Related Annealing Phenomena" (Pergamon Press, 1995).
17. G. M. VYLETEL, P. E. KRAJEWSKI, D. C. VAN AKEN, J. W. JONES and J. E. ALLISON, *Scripta Metall. et Mater.* **27** (1992) 549.
18. F. J. HUMPHREYS, *Acta Metall.* **25** (1977) 1323.
19. E. NES, *ibid.* **24** (1976) 391.
20. E. NES and J. A. WERT, *Scripta Metall.* **18** (1984) 1433.
21. J. W. CAHN, *Acta Metall.* **4** (1954) 449.
22. R. SANDSTROM, *Z. Metallkde* **71** (1980) 681.
23. E. E. UNDERWOOD, "Quantitative Stereology" (Addison Wesley, Reading, MA, 1970) p. 81.
24. M. FERRY, P. R. MUNROE and A. CROSKY, *Scripta Metall. Mater* **29** (1993) 741.
25. R. L. FULLMAN, *Trans. A.I.M.E.* **197** (1953) 447.
26. M. FERRY, P. R. MUNROE and A. CROSKY, *Scripta Metall. Mater* **29** (1993) 1235.
27. P. HERBST and J. HUBER, in Proc. 5th Int. Conf. on Textures, edited by G. Gottstein and K. Lücke, Berlin (1978) Vol. 1, p. 453.

Received 15 July 2002
and accepted 8 January 2003